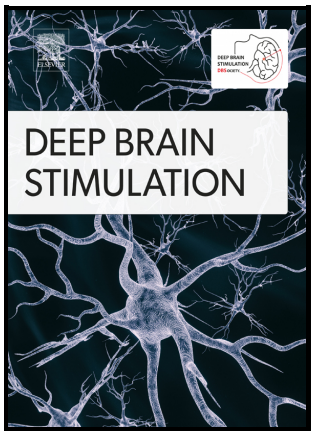

Patterns of Neural Activity and Clinical Outcomes in a Juvenile Huntington's Disease Patient Undergoing Deep Brain Stimulation of the Subthalamic Nucleus

Ahmet Kaymak, Matteo Vissani, Matteo Lenge, Federico Melani, Edoardo Fino, Pietro Cappelletto, Germana Tuccinardi, Michele Alessandro Cavallo, Flavio Giordano, Alberto Mazzoni

PII: S2949-6691(23)00002-7

DOI: https://doi.org/10.1016/j.jdbs.2023.03.001

Reference: JDBS3

To appear in: *Deep Brain Stimulation*
Revised date: 22 February 2023
Accepted date: 10

Please cite this article as: Ahmet Kaymak, Matteo Vissani, Matteo Lenge, Federico Melani, Edoardo Fino, Pietro Cappelletto, Germana Tuccinardi, Michele Alessandro Cavallo, Flavio Giordano and Alberto Mazzoni, Patterns of Neural Activity and Clinical Outcomes in a Juvenile Huntington's Disease Patient Undergoing Deep Brain Stimulation of the Subthalamic Nucleus, *Deep Brain Stimulation,* (2022) doi:https://doi.org/10.1016/j.jdbs.2023.03.001

Patterns of Neural Activity and Clinical Outcomes in a Juvenile Huntington's Disease Patient Undergoing Deep Brain Stimulation of the Subthalamic Nucleus

Ahmet Kaymak[1,2], Matteo Vissani[3,4], Matteo Lenge[5], Federico Melani[6], Edoardo Fino[6], Pietro Cappelletto[6], Germana Tuccinardi[7], Michele Alessandro Cavallo[8], Flavio Giordano[5], Alberto Mazzoni[1,2]

[1] The Biorobotics Institute, Scuola Superiore Sant'Anna, Pisa, Italy

[2] Department of Excellence for Robotics and AI, Scuola Superiore Sant'Anna, Pisa, Italy

[3] Department of Neurosurgery, Massachusetts General Hospital, Boston, United States of America

[4] Harvard Medical School, Boston, United States of America

[5] Department of Neurosurgery, Anna Meyer Children's Hospital, University of Florence, Florence, Italy

[6] Department of Neuroscience, Anna Meyer Children's Hospital, University of Florence, Florence, Italy

[7] Department of Neuroanesthesiology and Intensive Care Unit, Anna Meyer Children's Hospital, University of Florence, Florence, Italy

[8] Department of Neurosurgery, University Hospital S. Anna, University of Ferrara, Ferrara, Italy

Corresponding Author

Dr. Alberto Mazzoni,

The Biorobotics Institute of Scuola Superiore Sant'Anna, Viale Rinaldo Piaggio 34, Pontedera, Pisa, Italy

E-mail: alberto.mazzoni@santannapisa.it

Word Count: 1365

Conflict of Interest: The authors declared no competing interest and, no grants or funding sources associated with this work.

ABSTRACT

Background:

Huntington's disease (HD) is a hereditary neurodegenerative disease leading to cognitive and motor impairment. HD depends on basal ganglia dysfunctions, but the role of subthalamic nucleus (STN) neurons is not completely known. Drug-resistant motor symptoms of HD can be alleviated by neuromodulation of the basal ganglia through Deep Brain Stimulation (DBS) of STN. DBS target selection is supported by intra-operative microelectrode recordings (MER). MER have been previously used to characterize neural dynamics of STN in several movement disorders and can provide information on firing patterns underlying HD.

Methods:

We analyzed MER data acquired during bilateral DBS of STN in a juvenile HD female patient with hypokinetic motor symptoms (generalized dystonia, stiffness, and severe gait impairment). Firing patterns of STN in HD were characterized by isolating single neuron activities (n=23) and measuring their regularity, bursting, and oscillatory behavior. Multi-unit activity recordings spectrum was used to estimate the presence of network oscillations.

Results:

STN neurons displayed irregular dynamics and intense and sparse bursting. Only 3/23 neurons presented oscillatory activity. However, network oscillations were detected, in particular in the beta (12-30 Hz) band. After bilateral STN-DBS surgery, the Unified Huntington's Disease Rating Scale decreased from 60 to 54.

Conclusions:

The most salient difference between HD and other movement disorders in STN activity is the presence of a weakly synchronized oscillatory mode, in which oscillations are evident at the network level but not at the single neuron level.

Keywords: Deep Brain Stimulation (DBS), Movement Disorder, Juvenile Huntington’s Disease, Single Unit Activity, Subthalamic Nucleus (STN)

1. Introduction

Huntington's disease (HD) is a dominantly inherited neurodegenerative disorder characterized by progressive behavioral dysfunctions, cognitive impairment, and involuntary choreiform movements.[1] The hallmark of HD is atrophy and degeneration of medium spiny neurons within the corpus striatum[2], associated with neuropathological changes in other areas including the subthalamic nucleus (STN).[2] Briefly, the selective loss of striatal neurons increases the inhibitory drive of the globus pallidus externus (GPe) on STN. As the subthalamic nucleus becomes hypofunctional, the inhibitory effect of globus pallidus internus (GPi) on the thalamus is therefore lessened, resulting in chorea.[3] In terms of atrophy, there is a significant neuronal loss of around 20% in the STN of HD patients.[4]

Motor symptoms of HD can be improved by Deep Brain Stimulation (DBS) of the internal segment of the GPi[5,6] and STN[6]. The selection of the optimal target for DBS electrodes combines pre-surgical imaging and intra-surgical visual inspection of microelectrode recordings (MER) to monitor the distinctive basal ganglia nuclei's firing activity[7]. GPi-DBS procedures can improve total Unified Huntington's Disease Rating Scale (UHDRS) scores by 5.4% to 34.5%[8]. STN-DBS was performed only on one HD patient successfully ameliorating the HD-associated chorea but not choreatic symptoms (bradykinesia and rigidity) over a long period (>3 months)[6].

Here we will report a rare case of STN-DBS for juvenile HD. To shed light on the pathological neural activity underlying HD we extracted from MER and characterized offline the HD-related STN neuron discharge pattern at the single-neuron level and the network oscillations estimated by the analysis of Multi-Unit Activity.

2. Case Description

2.1 Patient Selection

This case reports a female juvenile patient affected by juvenile HD (Westphal variant), diagnosed when she was 6 years old, and symptomatic ever since. Familiarity is described in the paternal line (father and paternal grandmother, affected by the same disease, died at 43 and 50 years of age, respectively). Genetic analysis on gene IT5 (CR 4p16) confirmed a pathological C-A-G triplets amplification (up to 83 repetitions). To improve the movement disorder, consisting of severe extrapyramidal hypokinetic symptoms without choreiform dyskinesia (as expected in the juvenile variant of the disease), many drug therapies were attempted (Xenazine, L-DOPA, Carbi-DOPA, Valproic Acid, and Clonazepam), without any satisfactory results. Therefore, when the subject was 13 years old, considering the clinical picture (bradykinesia, generalized dystonia, and stiffness), the absence of psychiatric symptoms, the progressive and disabling course of the disease and the suitable target anatomy (normal STN nucleus without anatomical damage), we performed bilateral STN-DBS surgery, in the aim of improving the motor hypokinetic symptoms and consequently ameliorating the daily activities autonomy.

2.2 Surgical Procedure

On the day of surgery, the Leksell stereotactic G frame (Elekta AB, Stockholm, Sweden) was placed with screws in the patient’s skull under general anesthesia. Induction was performed in spontaneous breathing with sevoflurane, the anesthesia plan was then deepened with propofol

(1-2 mg/Kg) and fentanyl (1-2 gamma/Kg) to allow the orotracheal intubation maneuver after topical anesthesia of the vocal cords with lidocaine. The maintenance of the anesthesia was carried out thanks to balanced anesthesia with sevoflurane (0.8-1 MAC) and remifentanil (0.15-0.25 mcg/Kg/minute). STN targeting was defined according to the anatomical location on MRI images and standard stereotactic coordinates relative to the midcommisural point (the line between the anterior and posterior commissure: 11.5 mm in the lateral, 2 mm in the posterior, and 4 mm in the ventral direction). Frame-based 1.5-T stereotactic MR-T1W images with Gd enhancement, plus MR-T2W images were performed. Two different trajectories were planned to enter on top of the frontal gyrus while avoiding ventricles and blood vessel penetration and targeting bilaterally the STN nucleus. Trajectories were planned with a stereotactic robot neurosurgical planning software (Neuroinspire, Neuromate, Renishaw-Mayfield, Chassieu, France). The same robotic device was used for the placement of the two electrodes under the neurosurgeon's control and coupled with the Leksell stereotactic G frame. For each hemisphere, after the optimal MER trajectory had been determined, fine localization of the DBS target was performed through online evaluation of MER (see subsection 2.3 for details). The DBS electrode (3389-40, Medtronic Inc., Minneapolis, MN, USA) was then implanted in the selected position. Subsequent implantation of the pulse generator (IPG) (Activa RC, Medtronic Inc., Minneapolis, MN, the USA) in the infraclavicular region was performed during the second step of surgery. On the first postoperative day, a computed tomography (CT) scan was conducted to check the proper electrode position and to rule out any complications (pneumocephalus, asymptomatic hemorrhages). The post-operative CT scan was overlapped and matched with the pre-operative MR including the aimed trajectories to STNs. The correct localization was verified both with anatomical and neuroradiological analysis.

2.3 Electrophysiological Recordings

As mentioned above, to optimize the proper localization of STN, MER was performed by using FHC microelectrodes (impedance=10 MOhm ± 1 MOhm (FC22670, Medtronic R, Minneapolis, MN)). As recommended by the standard surgical technique of DBS, the MER started 10 mm above the intended target and advanced with 0.5-mm steps by micro driver tool (FHC Neural-Microtargeting®; Bowdoin, ME USA) to 2.5 mm below the target, where the electrophysiological STN signal was lost. We used concurrent 3-track recordings with the planned trajectory as the central channel and additional lateral and anterior channels at a 2-mm distance from the central channel. Electrophysiological STN activity was recognized online as a typical broadening of background noise with tonic and irregular discharge patterns and occasional bursts.

Following MER acquisition, a microelectrode stimulation was started 10 mm above the intended target of STN using the same electrode to rule out the recruiting of motor pathway fibers hence avoiding any stimulation side effects. The optimal response to such stimulation consisted of a clinical effect on the contralateral limb's muscular tone as perceived by the neurophysiological by making a passive movement. This response indicates a correct localization of the electrode into the target.

3. Clinical Outcome

At the preoperative evaluation, the subject presented with hypokinetic motor symptoms such as generalized dystonia, stiffness, and severe gait impairment, and the Unified Huntington's

Disease Rating Scale (UHDRS) score was 60. Two weeks after surgery, when STN stimulation was initiated (1.5 V amplitude, 130 Hz frequency, 90 μs pulse width), UHDRS was comparable (61), showing no postoperative complications affecting motor symptoms. At the first-year evaluation, being the stimulation parameters 0.7 V amplitude, 130 Hz frequency, and 90 μs pulse width, we observed a slight clinical improvement, consisting of a decrease in dystonia and stiffness and an improvement in the motor initiative and gait autonomy (UHDRS score was 54). After 1 year of follow-up, due to the progression of the underlying disease, the subject developed several complications impairing the global clinical picture and unrelated to the initial DBS therapeutic effects (focal epilepsy, severe behavioral disorders, dysphagia with the necessity of PEG positioning) that significantly affected the evaluation of motor performances.

4. MER Processing and Statistical Analysis

Following MER acquisition, we performed an offline spike sorting procedure (see Supplementary Methods) to isolate (n=23) single-unit activities (SUAs). We extracted multiple temporal and spectral features from each SUA, including firing rate and regularity, bursting, and oscillatory dynamics (see Supplementary Methods Table 1).

Considering the whole set of neurons, the median firing rate was 10.39 spikes/second (inter-quartile-range 8.25-14.87), with a median coefficient of variation of 1.45 (inter-quartile-range 0.94-2.33) and a mean local variation of 0.81±0.29 (Figure 1A) (Table 1). Interestingly, bursts were short-lived (0.06±0.04 seconds) intense (intra-burst firing rate 217.48±143.87 spikes/second), and followed by long pauses (inter-burst interval duration 2.76±0.63 seconds) (Figure 1B). We checked for the presence of strong oscillations in all SUAs, independently from their specific firing pattern, following the procedures described in the Supplementary Methods. Most of the SUAs did not present strong oscillatory activity (20/23), and we only observed limited beta (12-30 Hz) (3/23) and low gamma (30-45 Hz) activity (1/23). We also compared the neural activity between the right and left hemisphere STNs, as well as the variations among neurons belonging to different discharge patterns. The neural activity was consistent across both hemispheres (Figure 1A-B). No neural activity feature exhibited a statistically significant difference ($p<0.05$, as determined through a Mann-Whitney U test with Holm-Bonferroni correction) between the two hemispheres. Finally, in both hemispheres, the activity was homogeneous along the dorsoventral axis (Kruskal-Wallis test on dorsal and ventral firing rate $p>0.05$ for splitting points z=-9, -11, and -13 in Montreal Neurological Institute (MNI) space, see Supplementary Methods Table 2).

We further classified neurons based on their firing regularity, defined as the logarithm of the scale parameters of the gamma function that is fitted to the distribution of inter-spike intervals (ISI) for the selected neuron's spike train. Based on the firing regularity value, neurons were designated as bursting, irregular, and tonic[9] (Figure 1C-E). The proportion of irregular, tonic, and bursting neurons were 9/23, 6/23, and 8/23 respectively. Bursting, irregular and tonic neurons differed significantly in terms of neural firing features. As expected, the metrics of firing regularity, cv, and standard deviation of ISI, which reflect the degree of spiking irregularity, were significantly different between irregular and tonic neurons ($p=0.002$, $p=0.002$, and $p=0.004$, respectively, the Mann-Whitney U test with Holm-Bonferroni correction). Additionally, the mean firing rate and mean of the ISI distribution metrics for irregular and tonic neurons were found to be significantly different ($p=0.024$, $p=0.025$

respectively, the Mann-Whitney U test with Holm-Bonferroni correction). Lastly, tonic neurons were distinguishable from both irregular neurons (p=0.0020, Mann-Whitney U test with Holm-Bonferroni correction) and bursting neurons (p=0.0012, Mann-Whitney U test with Holm-Bonferroni correction) based on the skewness of the ISI distribution. Interestingly, no bursting neuron displayed strong oscillations, indicating that bursts were not periodic. Two irregularly firing neurons exhibited beta-oscillation patterns, while one tonic neuron displayed both beta and low-gamma oscillations intervals.

We complemented SUA analysis with the analysis of Multi-Unit Activity (MUA), i.e., the high-frequency portions (>300Hz) of extracellular activity in each MER (n=35)[10]. The low-frequency oscillatory segments of MUA, representative of the overall network activation, were analyzed by extracting their envelope[10,11]. After obtaining the low-frequency envelope of MUA, we assessed its oscillatory characteristics using the same methodology employed for SUA analysis. We observed strong beta band oscillations in 32/35 MUA recordings, all displaying a similar peak at around 22Hz. Additionally, alpha-band (8-12 Hz) and low gamma band oscillations were detected in 21/35 and 13/35 MUA recordings respectively. In contrast, neural oscillations in the delta (1-4 Hz) and theta (4-8 Hz) frequency ranges were uncommon and observed in only a small number of cases (n=8/35 and n=3/35 respectively).

5. Discussion

To our knowledge, we characterized STN single-neuron activity in a juvenile HD patient for the first time. Neurons exhibited short, intense, and sparse bursting but no prominent oscillatory activity at the single-neuron level. The firing rate and fraction of bursting neurons were similar to what was observed in Tourette Syndrome (TS) patients and lower than in Parkinson's Disease (PD) patients. Note that we considered only recordings performed under general anesthesia (GA) as our patient. Interestingly, SUA in our HD patient displayed no prominent oscillatory activity, as observed instead in TS and PD in the delta and beta bands respectively (Table 1). This indicates a lack of strongly synchronized oscillations in the STN of our patient. However, the same oscillation analysis applied on low-frequency envelopes of MUAs revealed notable oscillatory activity in the beta and alpha bands and, to a lesser extent, in the low gamma band. Overall, these results suggested the presence of weakly synchronized oscillations[12], i.e., a network oscillation that is not detectable at the single neuron level as each single unit participates only in a fraction of the oscillatory cycles.

Due to the rarity of HD, the literature on neural characteristics at the single-neuron level is limited. The majority of studies concentrate on the globus pallidum structures; the globus pallidus pars interna (GPi), and the globus pallidus pars externa (GPe). Furthermore, these studies primarily compare HD's neural dynamics with PD. Interestingly, no SUA-based analysis revealed evident oscillatory activity for individual neurons from GPi and GPe in HD, even under local anesthesia (LA)[13,14], which aligns with our results. However, our findings regarding the existence of bursting activity (39.1%) in the STN do not match with studies that have suggested that burstiness in pallidal neurons is rare or absent in HD[13,15].

In terms of local field potential (LFP) studies, there is varying information regarding the spectral characteristics of LFP recordings collected from HD patients. One study investigated the LFP of two juvenile HD patients (no prevalent chorea) who underwent bilateral GPi-GPe DBS under GA and remarked that globus pallidus activity shows spectral peaks at alpha and beta with no increased gamma band oscillation[16]. These findings are similar to what we report

here in the MUA envelope from STN of juvenile HD, with the exception that we did observe low gamma band oscillations. Two studies conducted on adult HD patients reported elevated spectral peaks in theta/alpha band (4-12 Hz)[17], low gamma (35-45 Hz)[17], and high beta–low gamma bands (26–43 Hz)[18].

A limitation in the interpretation of our results is the distortions of neural activity induced by sedative usage during the acquisition of MER recordings. Indeed, the use of sevoflurane for sedation has been found to cause a shift in beta and gamma band oscillations in the subthalamic nucleus towards lower frequencies in patients with PD[19,20]. However, this sedation was not found to affect the spike-bursting characteristics of subthalamic neurons, as compared to the awake condition[21]. There are conflicting results in the literature regarding the use of remifentanil for STN DBS surgeries in PD patients, which can be explained by the dose-dependent effects of the agent. Research suggests that at low doses, the discharge pattern of subthalamic neurons remained relatively stable during the recording duration, while higher doses resulted in an apparent reduction in beta and high-frequency oscillation (HFO) activity, which was not our case, and an increase in sub-beta band activity[22–24]. Therefore, our commentary regarding the low-frequency oscillations observed in MUA should be approached with caution, as the impact of sedatives on MER must be taken into consideration.

Finally, regarding the patient's condition, not only the improvement in UHDRS (which is more suited for adult HD) but also the improvements in generalized dystonia, stiffness, and severe gait impairment suggest that the STN DBS can ameliorate hypokinetic motor symptoms and gait autonomy for juvenile HD. Considering common use of DBS surgery for HD concentrates mainly on alleviating choreatic symptoms, our study investigated a new use of DBS for juvenile HD without chorea.

Statement of Ethics

The study was approved by the Regional Ethics Committee for Clinical Trials of Tuscany - Pediatric Ethics Committee section, (reference number 267/2022) and was carried out according to the Declaration of Helsinki. The patient's mother gave her consent to surgical procedures and scientific research on this issue.

Conflict of Interest Statement

The authors declared no competing interest associated with this work.

Funding Sources

This study was not supported by any funding sources.

Submission Declaration

This manuscript is a unique submission and is not being considered for publication, in part or in full, with any other source.

Data Availability Statement

The data that support the findings of this study are available on request from the corresponding author. The data are not publicly available due to privacy or ethical restrictions.

Authors' Roles

AK, MV, and AM contributed to the conception and design of the study, data analysis, interpretation, drafting, and revising of the article. FG, MAC, EF, PC, FM, and RG contributed to the conception and design of the study, data collection, interpretation, and revising of the article. ML contributed to the conception and design of the study, data collection, and interpretation.

References

1. Nance, M. A. Huntington disease: clinical, genetic, and social aspects. J Geriatr Psychiatry Neurol 11, 61–70 (1998).

2. Blumenstock, S. & Dudanova, I. Cortical and Striatal Circuits in Huntington's Disease. *Front. Neurosci.* **14**, 82 (2020).

3. Vonsattel, J. P. G., Keller, C. & Pilar Amaya, M. del. Neuropathology of Huntington's Disease. in *Handbook of Clinical Neurology* vol. 89 599–618 (Elsevier, 2008).

4. Guo, Z. *et al.* Striatal neuronal loss correlates with clinical motor impairment in Huntington's disease: Neuronal Loss And Motor Impairment in HD. *Mov. Disord.* **27**, 1379–1386 (2012).

5. Moro, E. *et al.* Bilateral globus pallidus stimulation for Huntington's disease. *Ann Neurol* **56**, 290–294 (2004).

6. Gruber, D. *et al.* Quadruple deep brain stimulation in Huntington's disease, targeting pallidum and subthalamic nucleus: case report and review of the literature. *J Neural Transm (Vienna)* **121**, 1303–1312 (2014).

7. Montgomery, E. B. Microelectrode targeting of the subthalamic nucleus for deep brain stimulation surgery. *Mov Disord* **27**, 1387–1391 (2012).

8. Bonomo, R. *et al.* Deep brain stimulation in Huntington's disease: a literature review. *Neurol Sci* **42**, 4447–4457 (2021).

9. Vissani, M. *et al.* Spatio-temporal structure of single neuron subthalamic activity identifies DBS target for anesthetized Tourette syndrome patients. *J. Neural Eng.* **16**, 066011 (2019).

10. Tepper, Á. *et al.* Selection of the Optimal Algorithm for Real-Time Estimation of Beta Band Power during DBS Surgeries in Patients with Parkinson's Disease. *Comput Intell Neurosci* **2017**, 1512504 (2017).

11. Bos, M. J. *et al.* Influence of Anesthesia and Clinical Variables on the Firing Rate, Coefficient of Variation and Multi-Unit Activity of the Subthalamic Nucleus in Patients with Parkinson's Disease. *J Clin Med* **9**, 1229 (2020).

12. Brunel, N. & Hakim, V. Fast global oscillations in networks of integrate-and-fire neurons with low firing rates. *Neural Comput* **11**, 1621–1671 (1999).
13. Tang, J. K. H. *et al.* Firing rates of pallidal neurons are similar in Huntington's and Parkinson's disease patients. *Exp Brain Res* **166**, 230–236 (2005).
14. Starr, P. A., Kang, G. A., Heath, S., Shimamoto, S. & Turner, R. S. Pallidal neuronal discharge in Huntington's disease: support for selective loss of striatal cells originating the indirect pathway. *Exp Neurol* **211**, 227–233 (2008).
15. Delorme, C. *et al.* Deep brain stimulation of the internal pallidum in Huntington's disease patients: clinical outcome and neuronal firing patterns. *J Neurol* **263**, 290–298 (2016).
16. Ferrea, S. *et al.* Pallidal deep brain stimulation in juvenile Huntington's disease: local field potential oscillations and clinical data. *J Neurol* **265**, 1573–1579 (2018).
17. Groiss, S. J. *et al.* Local field potential oscillations of the globus pallidus in Huntington's disease. *Mov Disord* **26**, 2577–2578 (2011).
18. Zhu, G. *et al.* Characteristics of Globus Pallidus Internus Local Field Potentials in Hyperkinetic Disease. *Front. Neurol.* **9**, 934 (2018).
19. Velly, L. J. *et al.* Differential dynamic of action on cortical and subcortical structures of anesthetic agents during induction of anesthesia. *Anesthesiology* **107**, 202–212 (2007).
20. Sinclair, N. C. *et al.* Electrically evoked and spontaneous neural activity in the subthalamic nucleus under general anesthesia. *J Neurosurg* 1–10 (2021) doi:10.3171/2021.8.JNS204225.
21. Tsai, S.-T., Tseng, G.-F., Kuo, C.-C., Chen, T.-Y. & Chen, S.-Y. Sevoflurane and Parkinson's Disease: Subthalamic Nucleus Neuronal Activity and Clinical Outcome of Deep Brain Stimulation. *Anesthesiology* **132**, 1034–1044 (2020).
22. Benady, A. *et al.* Sedative drugs modulate the neuronal activity in the subthalamic nucleus of parkinsonian patients. *Sci Rep* **10**, 14536 (2020).
23. Maciver, M. B., Bronte-Stewart, H. M., Henderson, J. M., Jaffe, R. A. & Brock-Utne, J. G. Human subthalamic neuron spiking exhibits subtle responses to sedatives. *Anesthesiology* **115**, 254–264 (2011).
24. Bos, M. J. *et al.* Effect of Anesthesia on Microelectrode Recordings During Deep Brain Stimulation Surgery: A Narrative Review. *Journal of Neurosurgical Anesthesiology* **33**, 300–307 (2021).
25. Vissani, M. *et al.* Spatio-temporal structure of single neuron subthalamic activity identifies DBS target for anesthetized Tourette syndrome patients. *J. Neural Eng.* **16**, 066011 (2019).

26. Myrov, V., Sedov, A., Salova, E., Tomskiy, A. & Belova, E. Single unit activity of subthalamic nucleus of patients with Parkinson's disease under local and generalized anaesthesia: Multifactor analysis. *Neuroscience Research* **145**, 54–61 (2019).
27. Hertel, F. *et al.* Implantation of electrodes for deep brain stimulation of the subthalamic nucleus in advanced Parkinson's disease with the aid of intraoperative microrecording under general anesthesia. *Neurosurgery* **59**, E1138; discussion E1138 (2006).
28. Lin, S.-H. *et al.* Subthalamic deep brain stimulation after anesthetic inhalation in Parkinson disease: a preliminary study. *J Neurosurg* **109**, 238–244 (2008).
29. Lin, S.-H. *et al.* Decreased Power but Preserved Bursting Features of Subthalamic Neuronal Signals in Advanced Parkinson's Patients under Controlled Desflurane Inhalation Anesthesia. *Front. Neurosci.* **11**, 701 (2017).
30. Lettieri, C. *et al.* Deep brain stimulation: Subthalamic nucleus electrophysiological activity in awake and anesthetized patients. *Clinical Neurophysiology* **123**, 2406–2413 (2012).

FIGURE LEGENDS

Figure 1. Neural features of subthalamic nucleus neurons in juvenile Huntington's Disease **(A)** Top row: Distribution of mean firing rate, firing regularity, coefficient of variation, local variation of all neurons in left (blue) and right (green) hemisphere. Bottom row: same for the mean of ISI, the standard deviation of ISI, skewness of ISI, and correlation coefficient of ISI Dots indicate neural features values of single neurons, while boxes and whiskers denote the 25^{th} to 75^{th} percentiles of the data and the variability outside the upper and lower quartiles (median ± 1.5 inter-quartile range) respectively. **(B)** Same as (A) for distribution of bursting features. **(C-E)** visualization of neurons belonging to different discharge patterns. **(C)** Properties of representative tonic neuron. Top left: action potential shape of single-unit activity (SUA), top right: raw (black) and SUA (red) components of MER recording, bottom left: the interspike-interval (ISI) distribution of spike train, bottom right: instantaneous firing rate (top) and raster plot (bottom). **(D)** same as (C) for a representative irregular neuron. **(D)** same as (C) for representative bursting neuron. Pink bars indicate bursts.

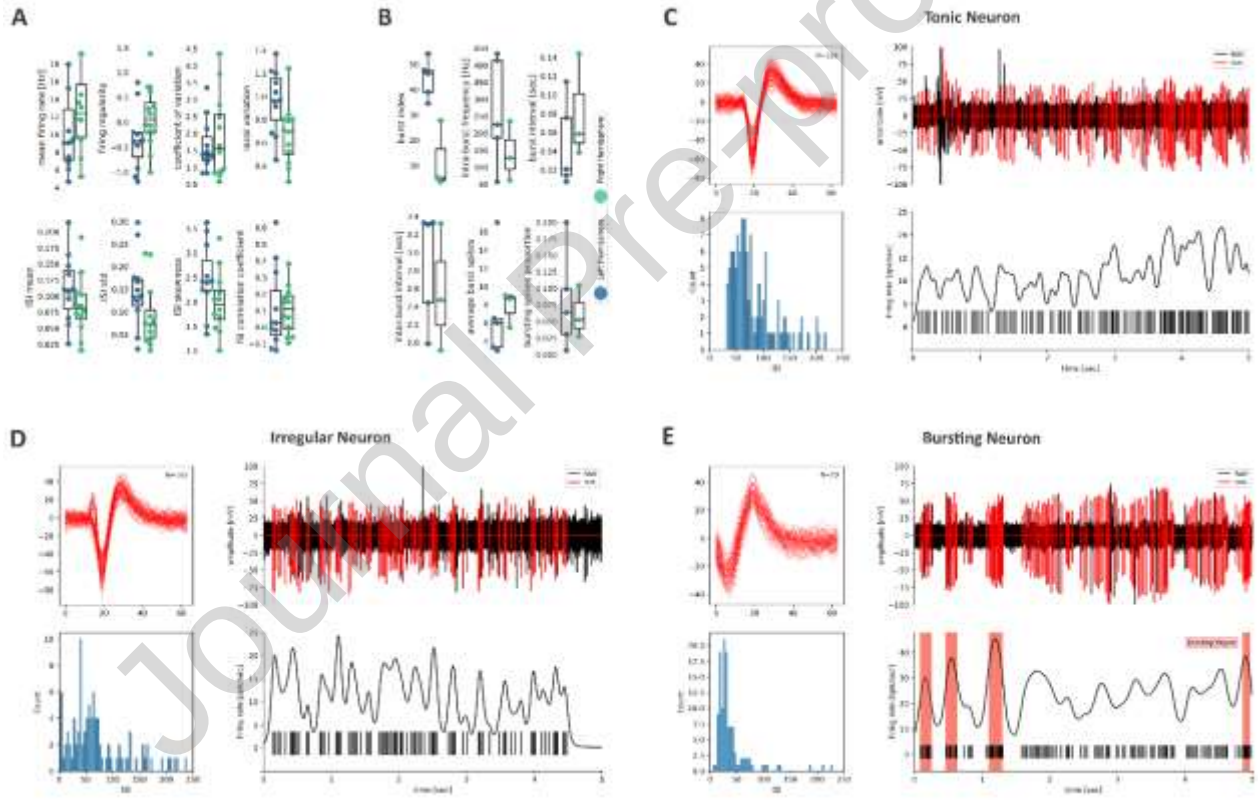

TABLE LEGENDS

Table 1. Comparison of STN SUA between present work and other movement disorders that have been published for DBS procedures that were carried out under general anesthesia

	Present Study (HD)	Parkinson's Disease	Tourette Syndrome
irregular (%)	39.13%		36.80%[25]
tonic (%)	26.09%		32.00%[25]
bursting (%)	34.78%	56.79%[26]	31.20%[25]
oscillatory (%)	13.63%		36.20%[25]
dominant frequency band	None	15-40 Hz[27]	1-4 Hz[25]
firing rate [spikes/second] median (25th -75th) or mean ± SD	10.39(8.25-14.87)	23.78[26] 29.7±14.6[28] 40[27] 35.394 ± 7.025[29] 24.0 ± 10.4 Hz[30]	12.2±6.1[25]
coefficient of variation median (25th -75th)	1.77(0.94-2.33)	2.29[26]	
local variation (mean ± SD)	0.81±0.29	0.69[26]	
anesthetics	propofol(1-2 mg/kg) and fentanyl (1-2 gamma/kg) the maintenance of the anesthesia was carried out with sevoflurane (0.8-1 MAC) and remifentanil (0.15-0.25 mcg/kg/min)	propofol 2-4 mg/kg/h[26] **induction**: 0.6 mg/kg rocuronium. **infusion**: 0.2-0.4 mg/kg/min propofol and 0.1-0.2 mg/kg/min remifentanil[27]	**induction**: 4 μg/kg remifentanyl and 0.5–1 mg/kg S(+) ketamine **infusion**: 0.25–1 lg/kg/min remifentanyl and 0.5– 3 mg/kg/h S(+) ketamine

Declaration of interests

☒The authors declare that they have no known competing financial interests or personal relationships that could have appeared to influence the work reported in this paper.

☐The authors declare the following financial interests/personal relationships which may be considered as potential competing interests: